

## **Effect of Sulphide Addition to Chloride Environment on Corrosion Behavior of SAF2507 Duplex Stainless Steel**

Zhiyuan Zhu

Jiangsu University of Science and Technology, Materials Science and Engineering, Zhenjiang 212003

E-mail: [salanganzhu@163.com](mailto:salanganzhu@163.com)

*Received:* 5 September 2016 / *Accepted:* 23 October 2016 / *Published:* 10 November 2016

---

The effect of sulphide addition to chloride environment on corrosion behavior of SAF2507 stainless steel at different temperatures was studied by slow strain rate test and electrochemical test, the tensile fracture morphology was observed by SEM. The results indicated that sulphide could enhance the stress corrosion susceptibility of SAF2507 duplex stainless steel. In addition sulphide made the general corrosion resistance of SAF2507 duplex stainless steel decrease. With the increase of temperature the effect of sulphide on rising corrosion susceptibility of steel was more obvious. In addition, sulphide made corrosion pits occurred in ferrite-austenite phase boundaries become increasing.

---

**Keywords:** SAF2507 Duplex Stainless Steel; Sulphide; Stress corrosion cracking; Electrochemical corrosion;

### **1. INTRODUCTION**

SAF2507 super duplex stainless steel was developed in the 1980s. It has two kinds of microstructures (ferrite phase and austenite phase), the volume ratio of ferrite phase and austenite phase is about 1:1 generally, and the minimum content of the two phases is also required up to 30% at least. The Pitting Resistance Equivalent Number (PREN) of SAF2507 super duplex stainless steel is greater than 40[1], so SAF2507 super duplex stainless steel achieves the considerably high resistance to pitting corrosion [2-4]. SAF2507 is highly alloyed duplex stainless steel and it has many excellent properties such as good resistance to chloride stress corrosion at high temperature [5-6], high strength, good welding performance and toughness, so SAF2507 duplex stainless steel is widely used in pulp mill equipments including clarifiers, accumulators, kraft digester and white liquor storage tanks, but corrosion and stress corrosion cracking are still major problems in the pulp and paper industry [7]. For example white liquor used in the kraft pulping process contains the highest concentrations of sodium

sulphide compared with other pulp mill liquors [8], hence white liquor is considered to be the most aggressive of all pulping liquors. Prior work has shown that sulphide species in white liquor may accelerate the corrosion of mild steel [9]. Wensley et al. have reported that raising the amount of sulphide can cause a decrease in the corrosion potential of mild steel in white liquor [10]. However, there is few work concerns on the effect of sulphide on corrosion behavior of SAF2507 duplex stainless steel. In addition, recent failures of DSS pulp mil equipment have made it is necessary to investigate the sulphide-containing solution that can lead SAF2507 to become sensitive to general corrosion and stress corrosion cracking. In order to make SAF2507 duplex stainless steel be more effectively applied, we should study the corrosion resistance property of SAF2507 duplex stainless steel, when it is in corrosion environment containing different levels of sulphide.

This paper presents the results of slow strain rate test and electrochemical test of SAF2507 duplex stainless steel in chloride environment with and without different levels of sulphide content at different temperatures. Besides the distribution of corrosion pits of SAF2507 in chloride environment and sulphide-containing chloride environment was also been observed.

## 2. EXPERIMENTAL

### 2.1 Experimental material

The material used in the study was SAF 2507 (UNS 2750) super duplex stainless steel with composition 0.021 C、 0.053 Si、 0.97 Mn、 0.001 S、 0.025 P、 25.02 Cr、 7.13 Ni、 3.7 Mo、 0.27 N (wt.%).

### 2.2 Slow strain rate test (SSRT)

Slow strain rate tests were carried out on SCC-1 stress corrosion testing machine. The size of the specimens was shown in Fig.1.

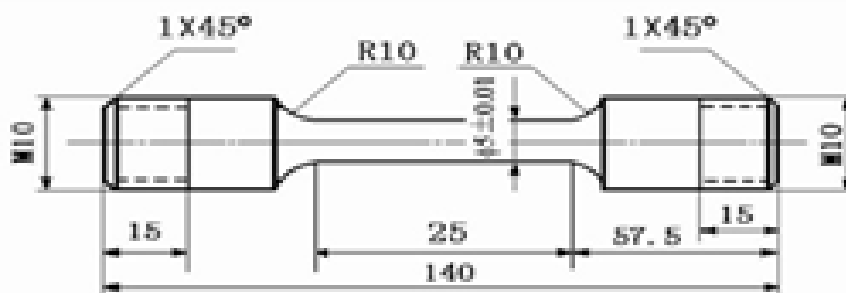


Figure 1. The size of SSRT sample

All surfaces of the specimens, except the gauge section were insulated with silicone casing. The strain rate was  $1 \times 10^{-5}$  mm/s. The tests were carried out in the air, 3.5% NaCl solution, 3.5% NaCl + 0.005M Na<sub>2</sub>S and 3.5% NaCl + 0.05M Na<sub>2</sub>S solution at room temperature.

### 2.3 Electrochemical test

Electrochemical tests were carried out on Gamry Reference 600 electrochemical workstation. The three-electrode cell was used in potentiodynamic anodic polarization curve measurement. The working electrode of the DSS samples had a diameter of 1cm and height of 1cm, and was embedded in epoxy resin, polished to diamond finish (1.5 $\mu$ m), rinsed in acetone and dried in the hot air before each experiment, the saturated calomel electrode (SCE) was reference electrode and platinum foil was counter electrode. Scan range was -0.2V-1.5 V (vs the open circuit potential) and scan rate was 1mV/s. The experiments were carried out in 3.5% NaCl solution, 3.5% NaCl + 0.005M Na<sub>2</sub>S and 3.5% NaCl + 0.05M Na<sub>2</sub>S solution at 20°C, 30°C, 45°C respectively. The AC singles of electrochemical impedance spectroscopy (EIS) measurements was 100 KHz to 3 mHz with the amplitude of 5 mV peak-to-peak.

Moreover, in order to study the corrosion morphology of SAF2507 DSS in 3.5% NaCl and 3.5% NaCl solution containing 0.05M Na<sub>2</sub>S at 20°C, the two specimens were electrochemically etched with 4M sodium hydroxide (NaOH) for approximately 30 seconds at a voltage of 2V DC and rinsed thoroughly with water and acetone, followed by air drying. Lastly, potentiodynamic anodic polarization tests were carried out in 3.5% NaCl and 3.5% NaCl containing 0.05M Na<sub>2</sub>S solution. After that optical examination was carried out to study the corrosion morphology.

### 2.4 Fracture and pitting corrosion morphology

Fracture morphology was observed after SSRT by SEM (ZEISS Merlin Compact). Pitting corrosion morphology was observed after the potentiodynamic anodic polarization measurements in 3.5% NaCl solution and 3.5% NaCl containing 0.05M Na<sub>2</sub>S solution at 20°C respectively by 3D Super Depth Digital Microscope (KEYENCE VHX-900).

## 3. RESULTS AND DISCUSSION

### 3.1 Slow strain rate test

#### 3.1.1 Stress-strain curve analysis

The stress vs. strain curves for SAF2507 duplex stainless steel in different conditions were shown in Fig. 2. It can be obtained from Fig. 2 that the tensile strength and fracture strain in the air were the largest but were decreased with the increase of sulphide content.

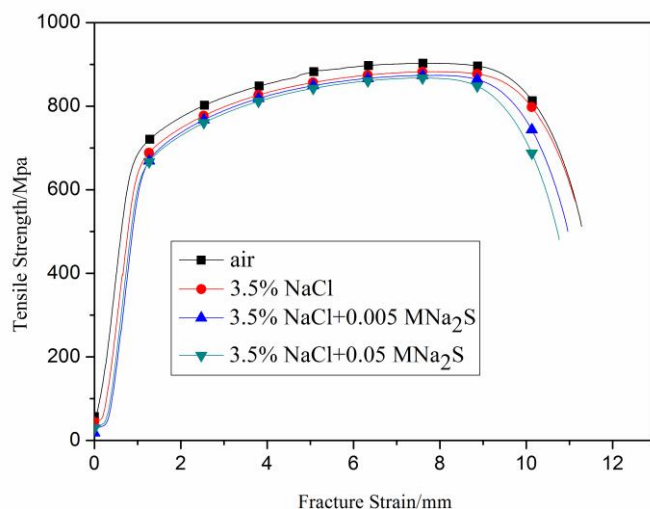


**Figure 2.** Stress vs. strain SSRT curves of SAF2507 stainless steel in 3.5%NaCl solution with different sulphide content at 20°C

**Table 1.** The SSRT results for SAF2507 duplex stainless steel in 3.5%NaCl solution with different sulphide content at 20°C

Environment	Tensile strength /MPa	Fracture strain/mm	Fracture time/h	$\sigma$	$\delta$	t
air	902.75	11.28	31.41	...	...	...
3.5%NaCl	882.66	11.13	31.33	0.02225	0.0133	0.00255
3.5%NaCl+0.005MNa <sub>2</sub> S	873.97	10.96	30.49	0.03189	0.0282	0.02929
3.5%NaCl+0.05MNa <sub>2</sub> S	867.51	10.76	29.93	0.03903	0.0460	0.04711

Moreover, from Table 1 we can obtained that fracture time was also decreased with the increase of sulfur ions content. All these mean that sulfur ions enhanced the stress corrosion cracking susceptibility of 2507 duplex stainless steel.

In this paper the index of  $\sigma$ 、 $\delta$ 、t were used to evaluate the stress corrosion susceptibility of SAF2507 duplex stainless steel[11].The value of  $\sigma$ 、 $\delta$  and t is higher, stress corrosion cracking sensitive of DSS2507 is bigger.

$$\sigma = (\sigma_0 - \sigma_1) / \sigma_0 \quad (1)$$

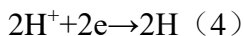
$$t = (t_0 - t_1) / t_0 \quad (2)$$

$$\delta = (\delta_0 - \delta_1) / \delta_0 \quad (3)$$

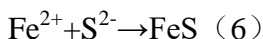
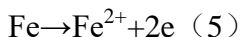
$\sigma_0$ ,  $t_0$  and  $\delta_0$  represents tensile strength, fracture time and fracture strain in the air, however  $\sigma_1$ ,  $t_1$  and  $\delta_1$  represents tensile strength, fracture time and fracture strain in the corrosion solution respectively. Table 1 shows that the value of  $\sigma$ 、 $\delta$  and t raises with the increase of Na<sub>2</sub>S content, which shows that sulphide can enhance the stress corrosion susceptibility of SAF2507 duplex stainless steel. In the condition of excluding sulfur ions, Cr in SAF2507 duplex stainless steel can combine with O<sup>2-</sup> or OH<sup>-</sup>

by ionic bonding generating a dense layer oxide film, whose composition is  $\text{Cr}_2\text{O}_3$  or  $\text{Cr}(\text{OH})_3$ . The oxide film can enhance the resistance to stress corrosion cracking property. But when sulfur ions exist in corrosion environment, sulfur ions can replace part  $\text{O}^{2-}$  or  $\text{OH}^-$  combine with  $\text{Cr}^-$ , which can destroy the integrity of oxide film on the surface of SAF2507. So for 2507 duplex stainless steel the capacity of resist stress corrosion cracking become weak. Moreover followings are cathode reaction and anodic reaction:

cathode reaction:



anodic reaction:



The sulfide formed during the anodic reaction can exist as other forms such as  $\text{FeS}_2$ 、 $\text{Fe}_3\text{S}_4$ 、 $\text{FeS}_{1-x}$  and so on. During the reaction process sulfur ions can reduce the binding force between atoms of steel, resulting in anodic dissolution occurring easily. Electrons generating in the anodic dissolution process can move to the surface of 2507 duplex stainless steel promote the formation of hydrogen atoms. Sulfide generated in the anodic reaction can absorb on the surface of steel, which result in hydrogen atoms were hard to re-assemble into molecular hydrogen spreading out [12-13]. Therefore hydrogen atoms penetrates into the steel concentrating in the defect and crack tip, which result in the capacity of resist stress corrosion cracking of 2507 duplex stainless steel become weak[14-15].

### 3.1.2 Tensile fracture morphology analysis

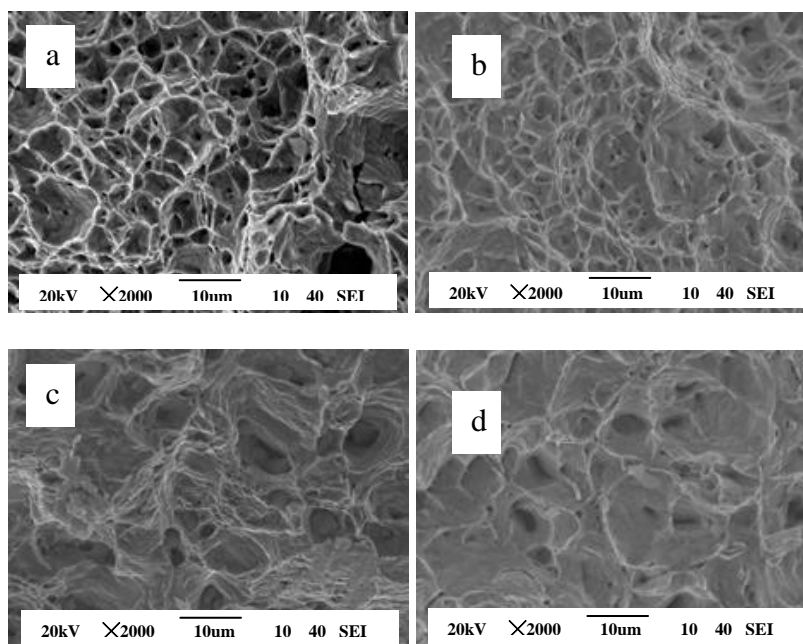


**Figure 3.** Tensile fracture SEM morphology of SAF2507 duplex stainless steel in 3.5%NaCl solution with different sulphide content at 20°C. (a) air, (b) 3.5%NaCl solution,(c) 3.5%NaCl+0.005M $\text{Na}_2\text{S}$  solution,(d) 3.5%NaCl+0.05M $\text{Na}_2\text{S}$  solution

Fig. 3 shows the tensile fracture SEM morphology of SAF2507 duplex stainless steel in different solutions. The tensile fracture SEM morphology of SAF2507 duplex stainless steel in the air owns obvious dimples and the number of them is large. SAF2507 duplex stainless steel presents obvious ductile fracture in the air. But with the addition of sulphide the number of dimple decreases and tensile fracture becomes flush, the ductile fracture characteristic become weak. So sulfur ions enhance the stress corrosion susceptibility of SAF2507 duplex stainless steel.

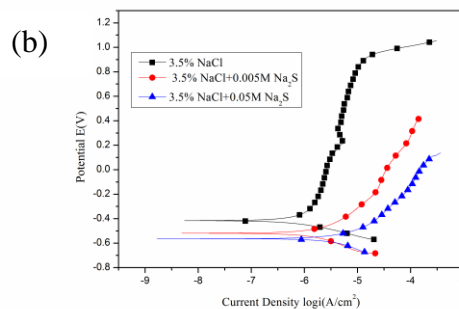
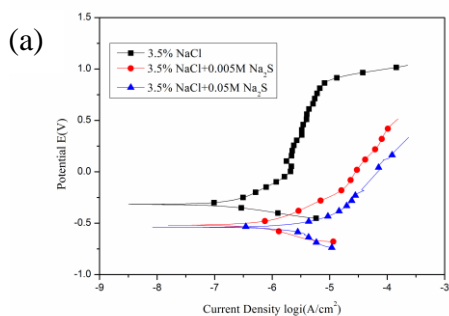
### 3.2 Electrochemical test

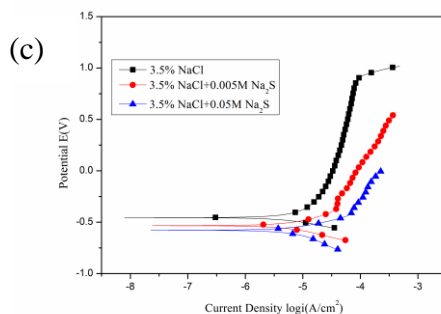
#### 3.2.1 potentiodynamic polarization curve test

The potentiodynamic polarization behavior for SAF2507 duplex stainless steel in 3.5% NaCl solution, 3.5% NaCl + 0.005M Na<sub>2</sub>S and 3.5% NaCl + 0.05M Na<sub>2</sub>S solution at 20°C, 30°C and 45°C was shown in Fig. 4 respectively, Tafel fitted results were shown in Table 2.

**Table 2.** Corrosion current density and corrosion potential for SAF2507 duplex stainless steel in 3.5%NaCl solution with different sulphide content at different temperatures

Temperature (°C)	Solution	Corrosion potential (V vs.SCE)	Corrosion current density (A/cm <sup>2</sup> )	Tafel slope (Anodic) (mV/dec)	Tafel slope (Cathodic) (mV/dec)
20	3.5%NaCl	-0.336	1.14×10 <sup>-7</sup>	621	152
	3.5%NaCl+0.005MNa <sub>2</sub> S	-0.513	1.21×10 <sup>-6</sup>	456	147
	3.5%NaCl+0.05MNa <sub>2</sub> S	-0.539	1.91×10 <sup>-6</sup>	423	150
30	3.5%NaCl	-0.416	6.85×10 <sup>-7</sup>	815	155
	3.5%NaCl+0.005MNa <sub>2</sub> S	-0.519	3.99×10 <sup>-6</sup>	625	148
	3.5%NaCl+0.05MNa <sub>2</sub> S	-0.564	6.83×10 <sup>-6</sup>	563	145
45	3.5%NaCl	-0.456	3.07×10 <sup>-6</sup>	913	142
	3.5%NaCl+0.005MNa <sub>2</sub> S	-0.533	8.27×10 <sup>-6</sup>	767	146
	3.5%NaCl+0.05MNa <sub>2</sub> S	-0.578	1.17×10 <sup>-5</sup>	653	148

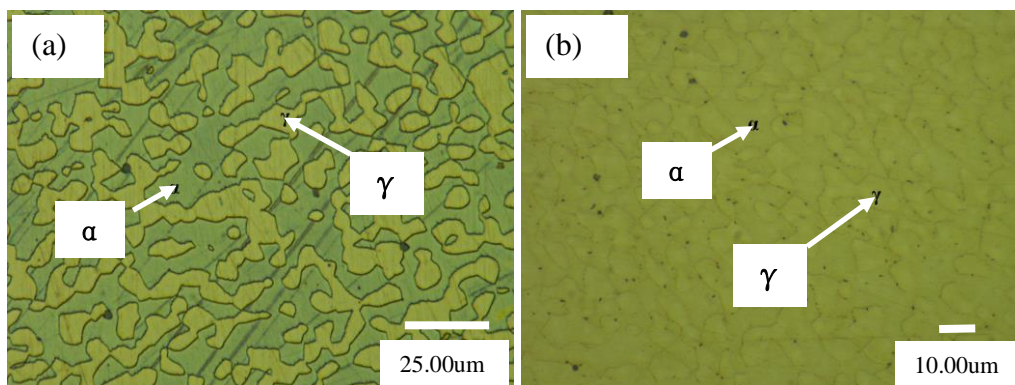




**Figure 4.** Potentiodynamic polarization curves of SAF2507 duplex stainless steel in 3.5%NaCl solution with different sulphide content at different temperatures. (a)20°C, (b) 30°C, (c) 45°C

From Fig.4, the anodic polarisation behavior of SAF2507 in 3.5% NaCl solution at different temperatures is different from that in sulphide-containing 3.5% NaCl solution. In 3.5% NaCl solution polarization curve exhibits a broad range of passivation, but in 3.5% NaCl solution containing different levels of sulfur ions content there is no passivation. Table 2 clearly indicates that the addition of sulphide to 3.5% NaCl solution causes a decrease in the corrosion potential and an increase in the corrosion current densities at different temperatures, which shows the detrimental effect of sulfur ions on the passivation behavior and corrosion susceptibility of SAF2507 duplex stainless steel. The anodic tafel slopes decrease with  $S^{2-}$  concentration increase, which means the passivation decrease with  $S^{2-}$  concentration increase. And the cathodic tafel slopes have no change, which indicate that  $S^{2-}$  concentration have no effect on cathodic reaction. It also can be obtained from Fig. 4 and Table 2 that in sulphide-containing 3.5% NaCl solution environment, an increase in temperature decreases the corrosion potential of SAF2507 duplex stainless steel and increases the corrosion current density, which indicates that it is difficult for SAF2507 to attain passivation in these solutions. The electronegativity of sulfur ions is strong and it can adsorb on the metal surface [16], which prevents the substances that are helpful for metal form passivation including  $O_2$ ,  $OH^-$  and so on from closing to metal surface. Therefore, the growth of passive film become slow. In addition, the existence of sulfur ions may destroy the structure of passive film on SAF2507 DSS surface and decrease the corrosion potential of the system, accelerate the formation of uniform corrosion of SAF2507 DSS [17]. Thereby the existence of sulphide is detrimental to the formation of passive film and decrease the corrosion resistance of SAF2507 DSS. Furthermore, hydrogen ions generating during the electrochemical reaction process are reduced to hydrogen atoms by electronic released from anodic reaction. Parts of the hydrogen atoms combine into  $H_2$  and release out, the others adsorb on SAF2507 surface and dissolve into the metal by desorption, which makes this area become brittle and results in hydrogen embrittlement at last [14,18]. Due to the interaction of the two factors the corrosion resistance of SAF2507 duplex stainless steel is weak in sulphide-containing 3.5% NaCl solution. With the increase of sulphide content and temperature, corrosion resistance of SAF2507 duplex stainless steel decreases more obviously.

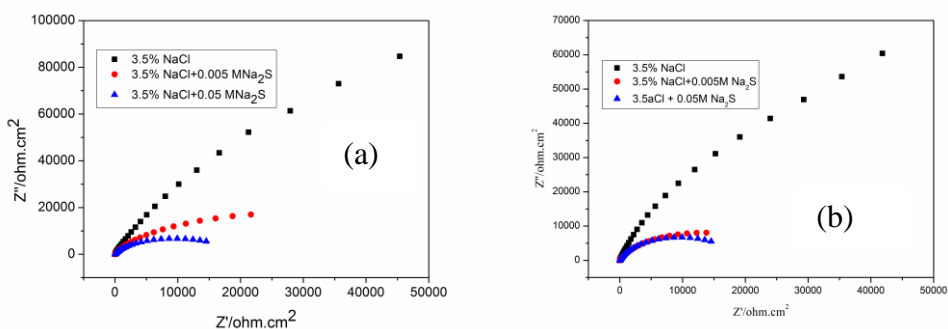
3.2.2 Corrosion morphology



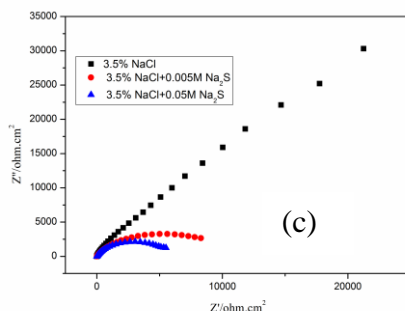
**Figure 5.** Corrosion morphology of SAF2507 duplex stainless steel after the potentiodynamic anodic polarization measurements (a):3.5%NaCl solution, (b):3.5%NaCl+0.05M Na<sub>2</sub>S solution (γ:austenitic phase; α:ferritic phase)

Fig. 5 shows the corrosion morphology of SAF2507 duplex stainless steel after the potentiodynamic anodic polarization measurements in 3.5% NaCl solution and 3.5% NaCl containing 0.05M Na<sub>2</sub>S solution at 20°C respectively. Darker phases present α-ferrite, the brighter phases are γ-austenite and the black spots are corrosion pits. Fig. 5 shows the number of corrosion pits in 3.5% NaCl solution is smaller than that in 3.5% NaCl containing 0.05M Na<sub>2</sub>S solution, which means sulphide decreases the corrosion resistance of SAF2507 duplex stainless steel and accelerates the corrosion process. In addition, it is evident that corrosion pits mainly distribute in ferrite phase in 3.5% NaCl solution, but in ferrite-austenite phase boundaries in 3.5% NaCl containing 0.05M Na<sub>2</sub>S solution from Fig.5. It is because that sulfur makes impurity segregate in ferrite-austenite phase boundaries preferentially [21].

3.2.3 EIS test







**Figure 6.** The Nyquist curves of SAF2507 duplex stainless steel in 3.5%NaCl solution with different sulphide content at different temperatures. (a) 20°C, (b) 30°C, (c) 45°C

The Nyquist plots for SAF2507 duplex stainless steel in 3.5% NaCl solution, 3.5% NaCl +0.005M Na<sub>2</sub>S and 3.5% NaCl +0.05M Na<sub>2</sub>S solution at 20°C, 30°C and 45°C were shown in Fig. 6 respectively. It can be seen from Fig. 6 that Z values (at different temperatures in 3.5% NaCl solution capacitive arc radius and polarization resistance) are all larger than that in sulphide-containing 3.5% NaCl solution. With the addition of sulphide capacitive arc radius and polarization resistance Z all decrease, which means sulphide enhances the corrosion susceptibility of SAF2507 duplex stainless steel. Faraday impedance mainly exists in the passive film firstly, however with the addition of sulphide a layer of sulfide film forms on SAF2507 surface and at this time the passive film on SAF2507 surface becomes thin [19]. When the sulphide content is high enough the passive film is completely destroyed resulting in Faraday impedance mainly existing in the sulfide film. The structure of sulfide film is not as compact as passive film, so impedance values decrease with the addition of sulphide. Besides it is evident from Fig.6 that in sulphide-containing 3.5% NaCl solution environment, with an increase of temperature capacitive arc radius decreases more obviously, which means the corrosion resistance of steel reduce [22].

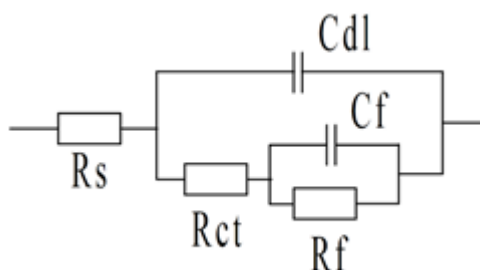


**Figure 7.** Equivalent circuit used for modeling the EIS results

Fig .7 shows the equivalent circuits used for modeling of obtained results [20]. Rs represents solution resistance, Cdl represents double layer capacitance, Rct represents the charge transfer

resistance, Cf represents passive film capacitor, Rf represents passive film resistance. The results of EIS method and calculated by Zsimpwin software were shown in Table 3.

**Table 3.** The results of EIS

Temperature (°C)	solution	Rct (ohm.cm <sup>2</sup> )	Rf (ohm.cm <sup>2</sup> )
20	3.5% NaCl	2760	$1.225 \times 10^5$
	3.5% NaCl+0.005MNa <sub>2</sub> S	1270	$2.121 \times 10^4$
	3.5% NaCl+0.05MNa <sub>2</sub> S	1320	$1.53 \times 10^4$
30	3.5% NaCl	1536	$7.6 \times 10^4$
	3.5% NaCl+0.005MNa <sub>2</sub> S	753.1	$1.104 \times 10^4$
	3.5% NaCl+0.05MNa <sub>2</sub> S	828	7516
45	3.5% NaCl	3884	$3.487 \times 10^4$
	3.5% NaCl+0.005MNa <sub>2</sub> S	2196	3290
	3.5% NaCl+0.05MNa <sub>2</sub> S	364.2	3571

Table 3 shows Rf in 3.5% NaCl solution is larger than that in sulphide-containing 3.5% NaCl solution at different temperatures, with the addition of sulphide Rf decreases in an order of magnitude. Therefore, it is obtained that sulphide can accelerate the anodic dissolution and reduce the corrosion resistance of SAF2507 [23]. In addition it is evident from table 3 that Rct decreases firstly and then increases slightly. With the addition of sulphide the passive film on SAF2507 surface is destroyed by sulfur ions and becomes thin gradually, so Rct decreases firstly; but when the passive film on SAF2507 surface is destroyed by sulfur ions completely, a layer of sulfide film forms on steel surface, the resistance for ion migration comes from the sulfide film, so Rct increases slightly again. However the overall trend of Rct is reduced. Moreover it also can be obtained from Fig.6 that the effect of sulphide on reducing Rf and Rct is more obvious with a rise of temperature. Hence, the increase of temperature is helpful for sulphide to decrease the corrosion resistance of SAF2507 duplex stainless steel [24]. In a word sulphide is detrimental to the corrosion resistance property of SAF2507 DSS, it enhances corrosion susceptibility and accelerates corrosion process of SAF2507 duplex stainless steel.

#### 4. CONCLUSIONS

(1) The stress corrosion cracking susceptibility of SAF2507 duplex stainless steel was enhanced by Sulfur ion. With the increase of sulphide content, the effect of sulphide on decreasing stress corrosion resistance is more obvious;

(2) Sulphide minifies the corrosion potential, passive film resistance and capacitive arc radius but improves corrosion current density; sulphide is detrimental to the general corrosion resistance of SAF2507 duplex stainless steel and with the increase of temperature the effect of sulphide on rising general corrosion susceptibility is more obvious;

- (3) Sulphide makes corrosion pits mainly distribute in ferrite-austenite phase boundaries.

#### ACKNOWLEDGEMENT

This work was financially supported by Natural Science Foundation of Jiangsu Province, China, (No. BK20141292), Science and Technology Support Program of Jiangsu Province (BE2015144) and Science and Technology Support Program of Jiangsu Province (BE2015145).

#### References

1. R. K. Singh Raman and W. H. Siew, *Corros. Sci.*, 42 (2010) 113.
2. Hua Tan, Yiming Jiang, Bo Deng, *Mater. Charact.*, 60(2009)1049
3. L.Q.Guo, M. Li, X.Li. Shi, Y Yan, X.Y. Li, L.J. Qiao. *Corros. Sci.*, 53(2011)3733
4. Chuanbo Zheng, Yanliang Huang, Qing Yu, *Corros. Eng. Sci. and Techn.*, 44(2009),96.
5. A. Girones, L. Llanes, M. Anglada and A. Mateo, *Int J Fatigue.*, 27 (2005) 197.
6. S. Shimodaira, M. Takano, Y. Taleizawa and H. Kamida, *NACE*, (1997) 1003.
7. C.Svensson , M.Pulliainen, M.Huttunen, P.Niemelainen, 2005 TAPPI Engineering, Pulping, Environmental Conference, Philadelphia, PA, USA, 2005
8. D. L. Singbeil and A. Garner, *Corros.*, 41 (1985) 634.
9. Z.Y.Liu, C.F.Dong, X.G.Li, Q.Zhi, Y.F.Cheng.. *J Mater Sci.*, 44 (2009)4228
10. D. A. Wensley and R. S. Charlton, *Corros.*, 36 (1980) 385.
11. R. Sánchez-Tovar, R. Leiva-García, J. García-Antón. *Thin Solid Films.*, 576 (2015) 1.
12. C. B. Zheng, B. H. Yan, K. Zhang and G. Yi, *Int. J. Min. Met. Mater.*, 22 (2015) 729.
13. C. B. Zheng, H. K. Jiang and Y. L. Huang, *Corros. Eng. Sci. Techn.*, 46 (2011) 365.
14. H. Chen, K. W. Gao, W. Y. Chu, Y. B. Wang and L. J. Qiao, *Acta Metall. Sin.*, 38 (2002) 857.
15. C. B. Zheng and Y. Guo, *Mater. Performance*, 50 (2011) 72.
16. A. Ikeda, S. Mukai and M. Ueda, *Corros.*, 4 (1995) 185.
17. A.M. Elhoud, N.C. Renton, W.F. *Inter. J. Hydrogen Energy*, 35(2010)6455
18. M. C. Zhao, Y. C. Shan, Y. H. Li and K. Yang, *Acta Metall. Sin.*, 10 (2011) 1090.
19. L. W. Liu, Q. Hu and F. Guo, *J. Chin. Soc. for corro. and protect.*, 22 (2002) 24.
20. G. L. Song, C. N. Cao and H. C. Lin, *J. Chin. Soc. for corro. and protect.*, 14 (1994) 113.
21. J. M. Cabrer, A. Mateo, L. Llana, J. M. Prado and M. Anglada, *J. Mater. Process. Technol.*, 143-144 (2003) 321.
22. A. Bhattacharya and P. M. Singh, *Corros. Sci.*, 53 (2011) 71.
23. C. B. Zheng, L. Cai, Z. J. Tang and X. L. Shen, *Surf. Coat. Tech.*, 287 (2016) 153.
24. Z. Fang, Y. Wu, R. Zhu, B. Cao and F. Xiao, *Corros.*, 50 (1994) 873.